TRANSIENT LAYERS OF ATMOSPHERIC METHANE ON MARS AFTER SURFACE RELEASE: A MODEL STUDY

S. Viscardy, F. Daerden, and L. Neary, *Royal Belgian Institute for Space Aeronomy, Brussels, Belgium (sebastien.viscardy@aeronomie.be)*

Introduction:

The presence of methane (CH4) on Mars has gained strong interest through repeated reports of its detection since 2003 [Formisano et al., 2004; Krasnopolsky et al., 2004; Mumma et al., 2009; Fonti and Marzo, 2010; Geminale et al., 2011; Krasnopolsky, 2012; Webster et al., 2015] and the possible implications for geophysical or biological activity on Mars. As methane is a reduced gas it is not stable in the highly oxidizing Martian atmosphere. Photochemical models have estimated that its lifetime is of the order of a few hundred years, assuming that the methane is destroyed only by the known photochemical processes [Summers et al., 2002]. As a result any presence of methane would point to more recent activity. One of the most likely sources for the atmospheric methane was that it was released from subsurface reservoirs by release through pores in the surface [Mumma et al., 2009].

The in-situ measurements by the Tunable Laser Spectrometer (TLS) of the Sample Analysis at Mars (SAM) on Curiosity represented a strong affirmation of the presence of methane on Mars in 2013-2014 [Webster et al., 2015], and showed a non-uniform trend of methane throughout the year, supporting the idea of intermittent methane release.

Until present nothing is known about the vertical distribution of methane at the times of any of the positive detections. Moreover GCM studies of surface release of methane focused on its horizontal spreading [Lefèvre and Forget, 2009; Mischna et al., 2011; Holmes et al., 2015]. However the upcoming ESA/Roskosmos ExoMars Trace Gas Orbiter (TGO) mission carries two instruments that are designed to measure the first vertical profiles of methane. These are the Nadir and Occultation for Mars Discovery (NOMAD) spectrometer suite [Vandaele et al., 2015] and the Atmospheric Chemistry Suite (ACS) [Korablev et al., 2015]. In anticipation of their measurements it is important to better understand the behavior of methane also in the vertical after an emission from the surface. This is the purpose of the present work in which we present some simple methane release experiments in a GCM and analyze the resulting vertical distribution of methane [Viscardy et al., 2016].

Model description:

The General Circulation Model for the atmosphere of Mars applied here is described in Daerden et al. [2015] and Viscardy et al. [2016]. It is a grid-point model based on the Canadian Global Environmental Multiscale (GEM) model for weather forecasting on Earth [Côté et al., 1998; Moudden and McConnell, 2005]. For the present study it was operated at 4°×4° horizontal resolution and with 102 vertical levels reaching from the surface to 8×10^{-6} Pa (~150 km).

The most important fields that govern the evolution of methane throughout the atmosphere after emission are the wind fields. As there are no global direct wind observations available for Mars, the simulations were evaluated with the Mars Analysis Correction Data Assimilation (MACDA) data set [Montabone et al., 2014]. The comparison is satisfactory both for the strength of the winds and for their distribution across latitude and height [Viscardy et al., 2016].

Results:

Because of the sparsity of the available methane observations the paper focuses on the qualitative evolution of the methane and avoids an exhaustive presentation of many possible emission scenarios. In the main simulation the emission was done at Nili Fossae (78°E, 22°N) at solar longitude Ls=150°, a choice inspired by the observations of Mumma et al. [2009]. This emission was found to be illustrative of emissions at other times and places and captured some of the most interesting behavior of methane after surface release. Initially the surface emission was assumed to be instantaneous, i.e. all methane was emitted during one model time step of 30 Mars-minutes (1/48 of a Mars solar day or sol), and the time of emission was local noon. The area over which the methane was released spanned one single grid cell measuring 4°×4° in latitude and longitude (~220 km × 237 km at the emission site). The amount of released gas was set at 5×10^{6} kg, i.e. ~30% of the total atmospheric mass of methane estimated by Mumma et al. [2009] for the 2003 event. The actual amount of emitted gas is not critical for the present study which only focuses on the qualitative aspects of the dispersion of the gas throughout the atmosphere. Initially it was also assumed that there is no methane present in the atmosphere at the time of the release. We investigated the evolution of the released methane on the course of twenty sols. For that reason, photochemistry or other loss processes were not taken into account.

The simulated horizontal evolution of the column-averaged mixing ratio of methane (the ratio of the vertically integrated number densities of methane and carbon dioxide) is plotted in Fig. 1 in steps of

five sols after emission. During the very first sols, the methane cloud moved mainly in a southwest direction up to a region centered around 60°E, 15°N (between Terra Sabaea and Syrtis Major) where it resided for several sols before a second component of the methane cloud developed east of the emission location which was well visible five sols after the release (Fig. 1a). Ten sols after release the bulk part of the cloud had gradually become less dense, while the eastern component of the methane cloud continued to develop eastwards just north of the equator (Fig. 1b). In the following five sols this evolution continued and the methane cloud had completed one turn around the planet along the equator (Fig. 1c). Twenty sols after emission, no indication of the location of the emission site remained (Fig. 1d). The meridional dispersion of the methane to higher latitudes was much slower than the zonal transport.

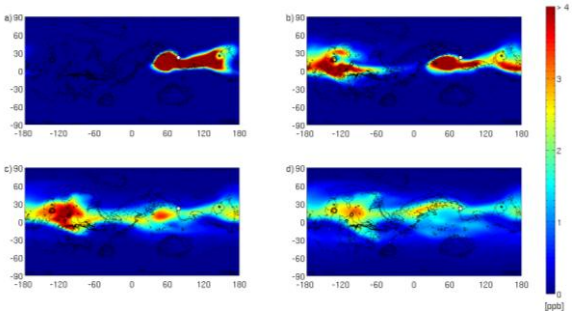

Figure 1. Horizontal distribution of the column averaged mixing ratio of methane (in ppb) for (a) five, (b) ten, (c) fifteen, and (d) twenty sols after an instantaneous surface release of methane in Nili Fossae (indicated by a white dot) at L_s = 150°.

Fig. 2 shows the simulated vertical evolution of the methane. To capture the three-dimensional evolution of the methane we provide plots of both zonally averaged volume mixing ratios (vmr) of methane (averaged over all longitudes, Fig. 2, left column) and meridionally averaged methane vmr (averaged over all latitudes, Fig. 2, right column). The zonal mean plots also show contour lines of the zonally averaged mass stream function as computed from the simulations, averaged over the 5 sols precedent to the time of the plot. This quantity is useful to understand the evolution of methane once it had ascended above the PBL. The meridional atmospheric circulation during the day differed strongly from that during the night and even had an opposite direction. When considering the net circulation over several days and nights, two main circulation cells of equal size appeared, one on either side of the equator (Fig. 2a,c,e,g). Their resulting effect was to lift the air from the lower atmosphere at low latitudes and to transport it upwards and to higher latitudes. The meridional mean plots have contour lines of the simulated zonal winds, averaged over the same time period, indicating the wind strength variation with height. These highlight the presence of strong zonal jets at 30-40 km height.

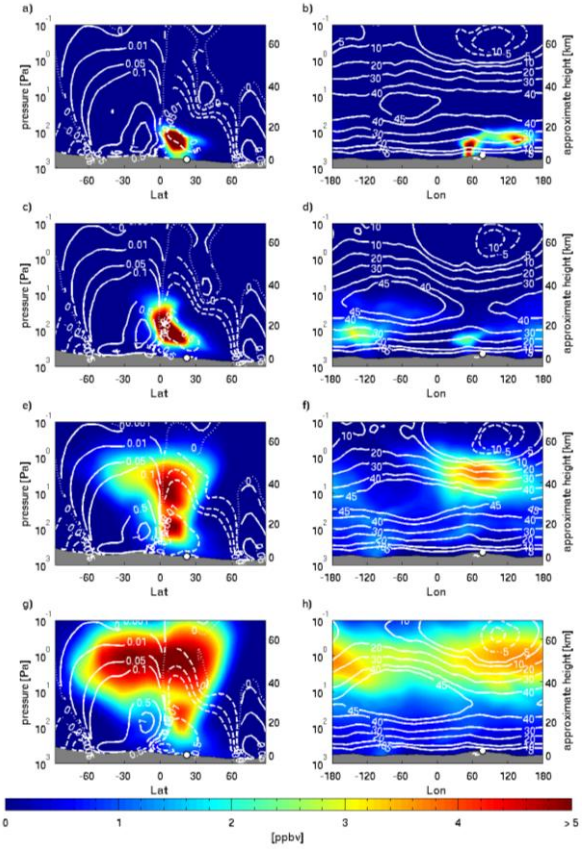

Figure 2. Vertical distribution of methane volume mixing ratio (vmr) in ppbv for five (a, b), ten (c, d), fifteen (e, f), and twenty sols (g, h) after the surface emission at Nili Fossae (indicated with a white dot). The left column (a, c, e, g) shows zonal mean methane vmr with contour lines of the mass stream function (×10^9 kg/s) zonally averaged over the planet and over the 5 preceding sols. Full lines represent counterclockwise movement and dashed lines represent clockwise movement of air. The right column (b, d, f, h) shows meridional mean methane vmr with contour lines added of the zonal component of the wind fields averaged over all latitudes and over the five preceding sols. Westerlies and easterlies are respectively represented by the full and dashed lines.

After release at local noon, the methane was rapidly mixed in the vertical due to the turbulent convection in the PBL and reached the top of the PBL (~11 km) around 3 p.m. When the PBL turbulence decreased in the late afternoon, the methane distribution remained steady with a slow descent at night as the atmosphere cooled down. As reported above, the released methane drifted to the southwest during the first few sols. By five sols after emission, part of the methane had risen to above the top of the PBL due to the upwelling branch of the Hadley circulation (Fig. 2a). Due to the differential advection and the westerly winds, the methane was drawn out in a layer at

~15 km height in a direction east of the emission location (Fig. 2b), explaining the eastern outflow reported above (Fig. 2a). Over the next five sols the methane continued to ascend above the equator following the streamlines (Fig. 2c) while it continued to move eastward (Fig. 2d). Fifteen sols after the release, the methane had reached heights up to 40 km where the zonal jets were of maximal strength and the dispersion process accelerated. The vertical distribution of the methane vmr was still highly non-uniform and showed distinct detached vertical layers (Fig. 2e,f). At the end of the first twenty sols, the methane started to become more dispersed towards higher latitudes following the streamlines (Fig. 2g) and had completed over one circle around the planet (Fig. 2h). As the atmospheric circulation dispersed the methane further over the next weeks, the distribution of methane became gradually more uniform over the entire atmosphere.

The mechanism described above is general and occurs in many cases. Results from a second simulation are shown in Fig. 3a, in which the same amount of methane (5×10^6 kg) was released from 240°E, 45°S at LS = 220°, a region and time of year where methane was reported to have been detected in 2005 [Mumma et al., 2009]. At this season (southern spring) two main circulation cells controlled the meridional transport: a small cell in the southern hemisphere and another much larger cell which transported the air from the southern to the northern hemisphere. After methane was released from the surface at latitude 45°S, the southern cell moved the methane slightly to the north until it reached ~40°S, which corresponded to the latitude of the intersection between the two major circulation cells. Then methane was gradually lifted upwards and moved northwards following the largest circulation cell. Twenty sols after release, distinct layers of methane were present in the atmosphere, roughly following the streamlines of the circulation cells (Fig. 3a), up to heights of 40 km. Most strikingly, the methane had moved to the northern hemisphere, remote from the emission location at 45°S.

In general, the fate of methane after release will be governed by the actual global circulation pattern at the place and time of the emission. It will follow the upwelling branches of the Hadley circulation cells and its spread along longitudes will speed up if it encounters strong zonal jets at typically 40 km height. Nevertheless there are also examples of emissions which do not lead to a dispersion throughout the atmosphere and the formation of layers. E.g. the circulation in the polar region during local summer is such that any methane that is released there will remain in the polar region. A third simulation was performed where 5×10^6 kg of methane was released from the surface at 240°E, 80°N at LS = 170° (late summer), a time and place suggested as a possible source of methane from analysis of measurements by PFS [Geminale et al., 2011]. Fig. 3b shows the distribution of methane after twenty sols, barely any methane had left the polar region and remained constrained to below 20 km.

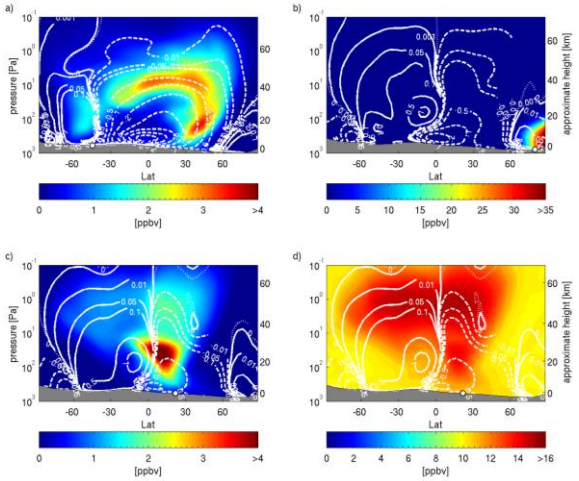

Figure 3. Zonal mean vmr of methane twenty sols after surface release for several simulations. (a) Instantaneous release from 240°E, 45°S at LS = 220°. (b) Instantaneous release from 240°E, 80°N at LS = 170°. (c) Continuous release over ten sols from 78°E, 22°N N at Ls=150°, in a pre-existent uniform background abundance of 10 ppbv. The emission site is indicated by a white dot in all plots. Contour lines of the mass stream function (×109 kg/s) are added as in Fig. 2.

In the previous simulations an instantaneous release of the total amount of methane was assumed, but the release could also be slow over a longer time period. The simulations were repeated but with methane continuously released with a constant flux over a period of ten sols, in the end accumulating to the same total amount of 5×10^6 kg. Fig. 3c shows the vertical distribution of methane twenty sols after the start of such a continuous release from Nili Fossae at Ls = 150°. When comparing with the case of an instantaneous release (Fig. 2g) the layers were less distinct at this time. The methane was dispersed similarly as the atmospheric circulation was identical, and the shape of the methane cloud is similar to that of the case of instantaneous release, but as the release lasted for a longer time with a lower flux, more methane is located at lower heights.

All these simulations were also repeated with a background of 10 ppbv of methane uniformly present in the atmosphere at the time of the emission. The resulting vertical distribution of methane for the instantaneous release from Nili Fossae is shown in Fig. 3d. The same patterns as for the simulation with zero background are reproduced (Fig. 2g) and the resulting distribution of methane was merely the sum of the pre-existing background and the released methane, i.e. the presence of a uniform background of

methane does not impact on the conclusions of our study.

Conclusions:

The NOMAD and ACS instruments on TGO are designed to provide the first vertical profile measurements of methane on Mars by applying the highly sensitive solar occultation technique [Vandaele et al. 2015; Trokhimovskiy et al. 2015]. They are planned to measure two vertical profiles per orbit at a latitude that varies smoothly throughout the Martian year [Vandaele et al., 2015]. With 12 orbits per day, for a specific day of the year, the TGO instruments will sample 24 profiles located at the same latitude with a spacing of ~15° in longitude. As our simulations show that methane released from the surface disperses rapidly over the planet, a daily sampling of 24 longitudes, even at a single latitude, will lead to a high likelihood of detecting a signature of any surface emission and will even allow the evolution of the released methane to be followed. GCM simulations can then be used to trace the methane back in time to confine the time of the release, if not the location of the source. Tracing methane emissions on Mars and locating their sources was originally foreseen to be the objective of the nadir IR channel of NOMAD [ESA, 2010; Zurek et al., 2011; Vandaele et al., 2015]. However the descope of a cryo-radiator due to mass constraints reduced the sensitivity of this nadir channel [Vandaele et al., 2015]. The present work shows how the solar occultation channel can complement the nadir channel for the monitoring of methane surface emissions. As the TGO instruments will not only measure methane but also temperature, dust, ice clouds and various chemical constituents including water vapor, the measurements can also help to investigate whether such methane layers originate from the dynamical process described in this report, or that they may possibly have another physical or chemical explanation, such as the evaporation of airborne methane clathrates [Chassefière, 2009].

References:

Chassefière, E., Metastable methane clathrate particles as a source of methane to the martian atmosphere (2009), Icarus, **204**, 137-144, doi:10.1016/j.icarus.2009.06.016.

Côté, J. et al. (1998), The Operational CMC MRB Global Environmental Multiscale (GEM) Model. Part I: Design Considerations and Formulation, Monthly Weather Review, **126**, 1373.

Daerden, F. et al. (2015), A solar escalator on mars: Self-lifting of dust layers by radiative heating. Geophys. Res. Lett., **42**, 1-8, doi:10.1002/2015GL064892.

Fonti, S., and G. A. Marzo (2010), Mapping the methane on Mars. Astron. & Astrophys., 512, A51, doi:10.1051/0004-6361/200913178.

Formisano, V. et al. (2004), Detection of Methane in the Atmosphere of Mars, Science, **306**, 1758-1761, doi:10.1126/science.1101732.

Geminale, A., V. Formisano, and G. Sindoni (2011), Mapping methane in Martian atmosphere with PFS-MEX data, Planet. Space Sci., **59** , 137-148, doi:10.1016/j.pss.2010.07.011.

Holmes, J. A., S. R. Lewis, and M. R. Patel (2015), Analysing the consistency of martian methane observations by investigation of global methane transport, Icarus, **257**, 23-32, doi:10.1016/j.icarus.2015.04.027.

Korablev, O. I. et al. (2015), ACS experiment for atmospheric studies on "ExoMars-2016" Orbiter, Sol. Syst. Res., **49**(7), 529-537.

Krasnopolsky, V. A., J. P. Maillard, and T. C. Owen (2004), Detection of methane in the martian atmosphere: evidence for life? Icarus, **172**, 537-547, doi:10.1016/j.icarus.2004.07.004.

Krasnopolsky, V. A. (2012), Search for methane and upper limits to ethane and SO2 on Mars, Icarus, **217**, 144-152, doi:10.1016/j.icarus.2011.10.019.

Lefèvre, F., and F. Forget (2009), Observed variations of methane on Mars unexplained by known atmospheric chemistry and physics, Nature, **460**, 720-723, doi:10.1038/nature08228.

Moudden, Y., and J. C. McConnell (2005). A new model for multiscale modeling of the Martian atmosphere, GM3, J. Geophys. Res. (Planets), **110**, 4001, doi:10.1029/2004JE002354.

Mischna, M. A. et al. (2011), Atmospheric modeling of Mars methane surface releases. Planet. Space Sci., **59**, 227-237, doi:10.1016/j.pss.2010.07.005.

Mumma, M. J. et al. (2009), Strong Release of Methane on Mars in Northern Summer 2003, Science, 323, 1041-1045, doi:10.1126/science.1165243.

Montabone, L. et al. (2014), The Mars Analysis Correction Data Assimilation (MACDA) Dataset V1.0, Geoscience Data Journal, **1**, 129–139, doi:10.1002/gdj3.13.

Summers, M. E. et al. (2002), Atmospheric biomarkers of subsurface life on Mars, Geophys. Res. Lett., **29**, 2171, doi:10.1029/2002GL015377.

Trokhimovskiy, A. et al. (2015), Middle-Infrared Echelle Cross-Dispersion Spectrometer ACS-MIR for the ExoMars Trace Gas Orbiter, Infrared Remote Sensing and Instrumentation XXIII, M. S. Scholl (Eds), 960808, doi:10.1117/12.2190359.

Vandaele, A. C. et al. (2015), Science objectives and performances of NOMAD, a spectrometer suite for the ExoMars TGO mission, Planet. Space Sci., **119**, 233-249, doi:10.1016/j.pss.2015.10.003.

Viscardy, S., F. Daerden, F., and L. Neary (2016), Formation of layers of methane in the atmosphere of Mars after surface release, Geophys. Rev. Lett., **43**, 1868-1875, doi:10.1002/2015GL067443.

Webster, C. R et al. (2015), Mars methane detection and variability at Gale crater. Science, **347**, 415-417, doi:10.1126/science.1261713.